

Electrophysiological Correlates for the Detection of Haptic Illusions

Yannick Weiss *Member, IEEE*, Albrecht Schmidt *Member, IEEE*, and Steeven Villa, *Member, IEEE*

Abstract—Haptic Illusions (HIs) have emerged as a versatile method to enrich haptic experiences for computing systems, especially in virtual reality scenarios. Unlike traditional haptic rendering, HIs do not rely on complex hardware. Instead, HIs leverage multisensory interactions, which can be elicited through audio-visual channels. However, the intensity at which HIs can be effectively applied is highly subject-dependent, and typical measures only estimate generalized boundaries based on small samples. Consequently, resulting techniques compromise the experience for some users and fail to fully exploit an HI for others. We propose adapting HI intensity to the physiological responses of individual users to optimize their haptic experiences. Specifically, we investigate electroencephalographic (EEG) correlates associated with the detection of an HI’s manipulations. For this, we integrated EEG with an established psychophysical protocol. Our user study (N=32) revealed distinct and separable EEG markers between detected and undetected HI manipulations. We identified contrasts in oscillatory activity between the central and parietal, as well as in frontal regions, as reliable markers for detection. Further, we trained machine learning models with simple averaged signals, which demonstrated potential for future in situ HI detection. These discoveries pave the way for adaptive HI systems that tailor elicitation to individual and contextual factors, enabling HIs to produce more convincing and reliable haptic feedback.

Index Terms—haptic illusions, physiological correlates, electroencephalography, stiffness perception.

I. INTRODUCTION

Haptic perception is fundamental to our ability to explore and interact with the physical world. However, integrating the full range of these sensations into computing systems remains a significant challenge, especially in virtual reality (VR) or extended reality (XR) environments where free-hand interaction is becoming increasingly prevalent. Simulating haptic properties such as stiffness, texture, and temperature often requires complex hardware systems, which can limit usability and scalability [1]. Haptic illusions (HIs) offer an alternative approach by leveraging the interplay between sensory modalities in shaping a unified perception of our environment [2, 3]. This allows one sensory input, such as vision or audition, to influence and partially override another, such as our haptic sense. HIs can exploit the integration of multisensory cues to modify the perceived haptic properties of objects, including their shape, size, weight, stiffness, texture, and temperature (cf. [4]). For example, synchronizing visual displacement and deformation cues with pressing rigid objects can evoke sensations of compliance [5, 6]. While effective, the success of HIs depends on maintaining congruency within specific perceptual

thresholds; excessive incongruency between sensory inputs disrupts integration and diminishes the illusion [7]. To mitigate this issue, HI research primarily relies on psychophysical experiments to quantify the approximate thresholds for detecting the incongruencies induced by HI [4]. The average detection thresholds derived from their sample size serve as rough estimates for the general population [8, 9, 10]. However, generalized thresholds cannot account for interpersonal variability, which compromises the experience for some users and fails to fully exploit the potential of the HI for others. This necessitates often impractical personalized procedures, e.g., via many repetitions using staircase methods.

To enhance individual calibrations, in this study, we investigate the use of physiological signals, specifically electroencephalography (EEG), to identify the detection of HI-induced incongruencies. EEG has demonstrated sensitivity to a range of phenomena related to sensory incongruencies [7, 11, 12, 13], making it a promising tool for identifying when the manipulation of an HI is detected. Using EEG alongside psychophysics methods, we aim to identify the neural correlates associated with HI detection and investigate how these could enable HIs to adapt to variations both within and across individuals.

Our study reveals distinct electrophysiological patterns for detected and undetected HI-induced incongruencies and demonstrates that EEG features can differentiate these states. This enables the development of personalized, adaptive systems that dynamically adjust HI elicitation based on individual and contextual factors, enhancing the effectiveness of haptic experiences.

II. RELATED WORK

This work draws from extensive research in haptic rendering, multisensory perception, and physiological measurements. Below, we provide a concise overview of haptic rendering techniques, haptic illusions, their perceptual boundaries, and suitable physiological correlates.

A. Haptic Rendering

Realistic haptic rendering has been identified as one of the principal challenges for virtual environments [1]. State-of-the-art systems primarily rely on vibrotactile actuators embedded in hand-held controllers, which cannot fully satisfy the large spectrum of haptic properties present in object interaction [14]. Consequently, research has brought forth numerous approaches for enabling haptic sensations in XR; for example, grounded robotic devices, such as the Touch X¹, Omega², or Falcon [15], render precise forces at high fre-

Yannick Weiss, Albrecht Schmidt, and Steeven Villa are with LMU Munich, 80337 Munich, Germany (email: {yannick.weiss, albrecht.schmidt, steeven.villa}@ifi.lmu.de).

¹<https://de.3dsystems.com/haptics-devices/touch-x>, accessed: 2025-05-22

²<https://www.forcedimension.com/products/omega>, accessed: 2025-05-22

quencies to produce accurate simulations of objects' kinesthetic properties. However, integrating these bulky devices in the environment and forcing users to constantly hold their end-effectors severely limits the interaction space in which they may be operated. Grounded and ungrounded encounter-type systems [16], such as robotic arms [17], have been proposed to extend the area for haptic rendering. However, these approaches tend to fall short regarding the precision and speed necessary to simulate a large variety of sensations while adding restrictions due to their sizes and energy requirements. Instead of augmenting the environment, many approaches aim to provide haptic feedback directly to the user through handheld devices [18] or wearables [19], ranging from bulkier exoskeletons [20] and haptic gloves [21] to finger-mounted devices [22]. These systems can each produce various haptic sensations, but they necessitate the implementation and constant carrying of additional hardware and impede natural object exploration by obstructing skin contact and limiting mobility. While active haptic systems continue to mature, research increasingly investigates HIs as an alternative that overcomes the restrictions inherent to hardware-based approaches.

B. Haptic Illusions

When we explore our environment, we rely on the simultaneous use of multiple senses, which evoke crossmodal interactions among them. This process is called multisensory integration [3]. Sensory illusions, including HIs, occur when information presented to distinct sensory modalities [3] — or subsystems within a modality, such as tactile and kinesthetic channels in haptics [22, 23, 24] — conflicts, causing the subjective perception to shift towards a percept trying to combine the conflicting stimuli. While HIs can occur naturally [25], evoking them deliberately has shown great potential for delivering haptic feedback [4]. By presenting controlled stimuli during haptic exploration to specific channels, such as vision or audition, HIs can induce modified haptic perceptions without necessitating additional haptic devices. This kind of haptic feedback is often referred to as pseudo-haptics, which was introduced by Lecuyer et al. [26] who showed that visual manipulation of spring deformations displayed on a screen could alter the perceived stiffness of a passive isometric input device. HIs have since been utilized to alter numerous haptic properties, including a virtual object's geometric properties, such as size and shape, or simulating material characteristics, such as weight, temperature, surface texture, and stiffness (refer to Kurzweg et al. [4] for a comprehensive review). They have been especially prominent in virtual environments, where the high control over users' auditory and visual sensations allows for large alterations of haptic experiences. Among them, we also find many approaches manipulating the proprioception of one's limbs using offsets in visual representation, which in turn has been used to extend the range of haptic experiences through redirection [27] or used to induce dynamic sensations of weight [28, 29] or stiffness [30, 8].

C. Perceptual Boundaries of Haptic Illusions

HIs offer many novel opportunities to generate and alter haptic experiences. However, their nature introduces innate

limitations; while multisensory integration enables the conflicting haptic and induced visual or auditory cues to form a unified percept, it breaks if the incongruities between the senses become too large [8]. In addition to impacting the efficacy of the HI, sensory conflicts may lead to discomfort or contribute to cybersickness [31]. To measure the breaking points or detection threshold of the induced incongruities, research generally relies on population-level approximations derived from controlled experiments on a small sample of participants. For instance, Tinguy et al. [10] and Auda et al. [32] respectively investigated how different a virtual object's shape and size can be displayed visually compared to its physical counterpart. Analogously, many works aim to estimate the perceptual boundaries of hand movement manipulations in mid-air [33, 34] or during haptic exploration, e.g., turning a knob [35] or pressing onto a compliant object [8]. These approaches generally follow classical psychophysical procedures for determining an average detection threshold of a predefined stimulus [36]. However, in addition to the effort required to scale these approaches to different HIs or more users, a single generalized threshold cannot account for individual interpersonal differences, which can be substantial in sensitivities to HIs [37, 38]. This either constrains the intensity of HIs to a very conservatively chosen threshold or creates noticeable breaks in multisensory integration for sensitive users.

D. Physiological Correlates to Sensory Incongruities

Psychophysical methods are effective for determining thresholds but are impractical for in-situ measurements due to the need for multiple repetitions before identifying a threshold (e.g., staircase methods). In contrast, physiological methods, particularly EEG, can measure neural potentials that are continuously triggered during the detection process, providing an alternative and complementary means of identifying sensed incongruities. Physiological measurements have become increasingly prevalent in interactive systems, particularly for VR [39]. Especially, EEG has demonstrated significant potential for capturing transient physiological processes due to its high temporal resolution, which makes it particularly well-suited for detecting rapid neural activity changes following stimulus onset [40, 7].

In the context of evaluating perceived incongruities in multisensory cue presentation, prior research has investigated various correlates of neural processes through EEG or similar screening methods. Göschl et al. [41] revealed contrasts in oscillatory power when participants were presented with congruent or incongruent visuo-tactile patterns rendered by a Braille stimulator and presented on a desktop screen. Further, Alsuradi et al. [42, 12] linked delayed rendering of haptic cues to changes in oscillatory activity and functional connectivity. Gehrke et al. [7] investigated temporal incongruities in virtual object interaction using vibrotactile and electro-muscular feedback, identifying Prediction-Error Negativity (PEN), a 100–200 ms deflection in Event-Related Potential (ERP), as a marker of mismatched multisensory cues, including poor haptic rendering. Similarly, Villa et al. [13] observed PEN

variations when visually presenting objects as gas, liquid, or solid while rendering them via mid-air ultrasound, attributing stronger mismatches for solids to limitations in simulating rigid kinesthetic feedback. Prediction Error (PE) and its modulation of cortical activity have additionally been prevalently studied during visuo-motor tasks, where visual incongruencies are introduced during cursor or limb movement [43, 44, 45]. Feick et al. [11] recently proposed EEG signals, combined with heart rate, movement data, and gaze information, to determine the personalized detection thresholds of hand redirections in virtual environments. They were able to separate movement amplifications at or above the subjective detection boundaries from congruent hand movements without visual manipulations. This signifies that physiological measures can partially identify inconsistent limb movements in virtual environments. However, the exploration has so far been limited to unrestricted mid-air hand movements, leaving the role of haptic components critical for HIs open for future research.

Overall, these investigations demonstrate the utility of physiological measurements for assessing perceived incongruencies in visuo-haptic rendering, spanning visuo-tactile, visuo-kinesthetic, and visuo-motor interactions. Yet, the use of EEG correlates to specifically identify the detection of HIs remains unexplored. To address this gap, we integrate EEG with an established psychophysical protocol to uncover electrophysiological correlates to the detection of incongruent stimuli produced by HI manipulations.

III. STUDY DESIGN

To assess EEG correlates to the reported detection of HIs on a comparative basis, we integrate our measurements to an established psychometric method for investigating detection thresholds [36]. Namely, we employ the Method of Constant Stimuli using a yes-no forced-choice paradigm. We presented different predefined levels of intensity of an HI and asked participants whether their multisensory experience was congruent.

Specifically, we largely replicated a typical setup for stiffness illusions [8, 22, 46]. In the current manuscript, we implemented a version closer to Weiss et al. [8], as this work addressed a visuo-haptic phenomenon for which thresholds have been widely investigated in multiple contexts [28, 33, 34]. While participants are pushing on a virtual object with constant stiffness in VR, we adjust the displacement movement of their virtual hand representation compared to their actual physical hand movements. By increasing or decreasing this movement ratio (called C/D RATIO), the virtual object can be made to be perceived as softer or harder, respectively. We record whether participants noticed this incongruency in hand movements by asking them the following question: *Did the movement of the virtual hand match the movement of your real hand during pressing?* Participants could only answer with *Yes* or *No*.

A. Participants

We recruited 32 participants through university mailing lists. 14 participants described themselves as female, 16 as male, and two as non-binary. Participants' age ranged from 20 to 66 ($M = 27.47$, $SD = 8.38$). 30 were right-handed, one

left-handed, and one unsure/ambidextrous. 27 participants had experienced VR before (13 below 2h, 11 between 2h and 20h, and 3 for more than 20h). All participants had normal or corrected-to-normal vision and no known conditions affecting the haptic acuity of the right hand. They were offered 10€ or university course credit as compensation. This study was approved by our institution's ethics board.

B. Apparatus

For the physical representation of the virtual object, we simulated a constant spring stiffness, i.e., applied forces increase linearly with displacement. For this, we employed a Novint Falcon haptic device [15], rendering appropriate forces at 1000Hz. We placed the Novint Falcon facing upwards on a table and connected a flat wooden 9cm×9cm square end-effector for participants to interact with. We attached a piece of paper to the surface of the end-effector to ensure a uniform texture. In the virtual environment, the end-effector is visually presented as a floating white cuboid with the same dimensions as its physical counterpart. Positional changes were tracked by the Novint Falcon and displayed at 90Hz on an HTC VIVE Pro head-mounted display (HMD). The virtual environment was constructed in Unity3D³ and ran on a Desktop PC with an NVIDIA GeForce RTX 3070 graphics card, a 12th Gen Intel Core i9 processor, and 32GB of RAM. The participant's right hand was tracked at 120Hz with an Ultraleap Leap Motion Controller⁴ and represented in the virtual environment by a low-poly model provided by Ultraleap. Participants held a presenter with two physical buttons in their left hand to answer the prompted questions. Additionally, we generated white noise on the HMD headphones to mask environmental noise or sounds caused by the haptic device. We acquired EEG signals at 500Hz through a 64-electrode R-Net EEG system⁵ from which we utilized 32 electrode channels. To synchronize the virtual environment and EEG, we employed the lab streaming layer (LSL) framework⁶. Figure 1 shows the setup used in our study.

C. Task

We tasked participants to press down and displace a virtual object by 30mm using the index finger of their right hand. This virtual object was physically co-located with the haptic device, rendering a constant spring stiffness of 363 N/m in line with previous investigations [26, 8]. When the haptic device's displacement reached the limit of 30mm, the virtual object turned green, signaling to the participants that they should remove their pressure. The object bounced back when participants lessened their applied force, analogous to a compression spring. We varied the C/D RATIO of the hand and object displacements during the entire press. After each press, the participants were prompted with the question: *Did the movement of the virtual hand match the movement of your*

³<https://unity.com/>, last accessed: 2025-05-22

⁴<https://www.ultraleap.com/>, last accessed: 2025-05-22

⁵Brain Products GmbH, Gilching, Germany, <https://www.brainproducts.com/solutions/r-net/>, last accessed: 2025-05-22

⁶<https://github.com/scn/labstreaminglayer>, last accessed: 2025-05-22

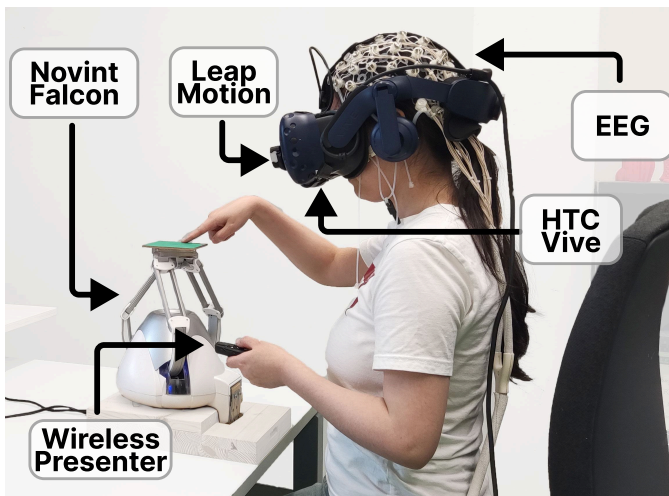


Fig. 1: Experimental setup integrating the EEG system, HTC Vive, Leap Motion Controller, Novint Falcon, and a wireless presenter for response input.

real hand during pressing? This question was shown in written form in front of the participants in the virtual environment. Beneath the question, we showed the two possible answers of *Yes* and *No*, which participants could select using the buttons of a wireless presenter they held in their left hand. After the selection, the next trial was started without feedback regarding the correctness of their answers.

D. Stimulus

We varied the C/D RATIO of physical to virtual hand movement as our independent variable. C/D RATIO generally describes the proportion of input (*Control*) to output (*Display*) movement of a user's action. While mapping the change in the virtual representation of users' movements, one-to-one is usually desired; prior works show that deliberately breaking this congruity can elicit altered sensations. For instance, Lécuyer et al. [47] simulated bumps and holes on a flat desktop screen by decreasing and increasing the ratio of physical mouse movement to visual cursor movement to induce sensations of inclined or declined slopes, respectively. In virtual environments, this approach is commonly implemented by altering the ratio of the actual movements of users' hands and the respective virtual movements of the hand representations in VR. Depending on the task and direction of movement, C/D RATIO adjustments showed to influence various related sensations, such as the weight of a lifted object [28, 29], the resistance of a knob being turned [35], kinesthetic forces when pushing an object [48], and the stiffness of virtual objects while pressing [8, 30].

As we aim to find electrophysiological correlates to the reported detection of incongruities introduced by these HI, we selected fixed levels of C/D RATIO according to the detection threshold study conducted by Weiss et al. [8]. We investigated four levels for each increased and decreased C/D RATIO in addition to baselines without ratio adjustments. Increased and decreased values were split into two blocks with a separate

baseline condition. The block for decreased C/D RATIO comprised $0\times$, $0.25\times$, $0.5\times$, $0.75\times$ and $1\times$ (baseline) the physical movement. The increased C/D RATIOS comprised $1\times$ (baseline), $2\times$, $3\times$, $4\times$, and $5\times$ the actual movement. Each C/D RATIO was repeated ten times, resulting in 50 trials per block. The two blocks were presented sequentially, and their order was counterbalanced among participants. Within each block, we randomized the trials.

E. Measures

To analyze the populous-level detection threshold using the established psychometric approach, we recorded participants' subjective responses (*Yes* and *No*) for each level of HI intensity. Further, using the R-Net EEG device, we recorded continuous EEG signals of the 32 channels and event markers for the start and end of the downward and upward phases of each press.

F. Procedure

We first informed participants about the study's procedure, apparatus, and aim. After obtaining their written consent, we asked them to complete a questionnaire regarding their demographics and previous experiences. Afterward, participants were seated in front of the study apparatus. Participants remained seated during the entire setup and experiment to reduce noise in the EEG data. We adjusted the chair and table height to position the haptic device's end-effector 10cm below the participant's shoulder height. The experimenter then attached the EEG system to the participant's head according to the international 10-10 electrode placement system. After ensuring each electrode's impedance level remained below $50\text{ k}\Omega$, the experimenter assisted the participants in putting on the VR headset. For each participant, the experimenter synchronized the virtual and physical positions of the end-effector using a VIVE Tracker. The participants are initially introduced to their task by three training trials, showing first a congruent and then a vastly exaggerated increased and decreased C/D RATIO to introduce them to the phenomenon they are tasked to judge. Afterward, the participants entered the experimental phase and completed all 100 trials sequentially without breaks. After finishing the study, the experimenter assisted the participants in taking off the VR headset and EEG. We provided shampoo, towels, and hairdryers for participants if they wanted to wash out the remaining saltwater applied for the EEG system. The overall duration of the experiment, including briefing and setup, was ~ 60 minutes.

G. EEG Preprocessing

We acquired EEG signals of 32 channels ($Fp1$, $Fp2$, $F9$, $F7$, $F3$, Fz , $F4$, $F8$, $F10$, $FC5$, $FC1$, $FC2$, $FC6$, $C3$, Cz , $C4$, $T7$, $T8$, $CP5$, $CP1$, $CP2$, $CP6$, $P9$, $P7$, $P3$, Pz , $P4$, $P8$, $P10$, $O1$, Oz , $O2$) at 500 Hz. We preprocessed and analyzed the EEG data using the Python MNE-library [49]. We first re-referenced the data to the average of all channels and applied a notch filter at 50 Hz to eliminate powerline interference, followed by a high-pass filter at 0.5 Hz and a low-pass filter at 35 Hz, following the methods described in previous work [50, 51]. Because we

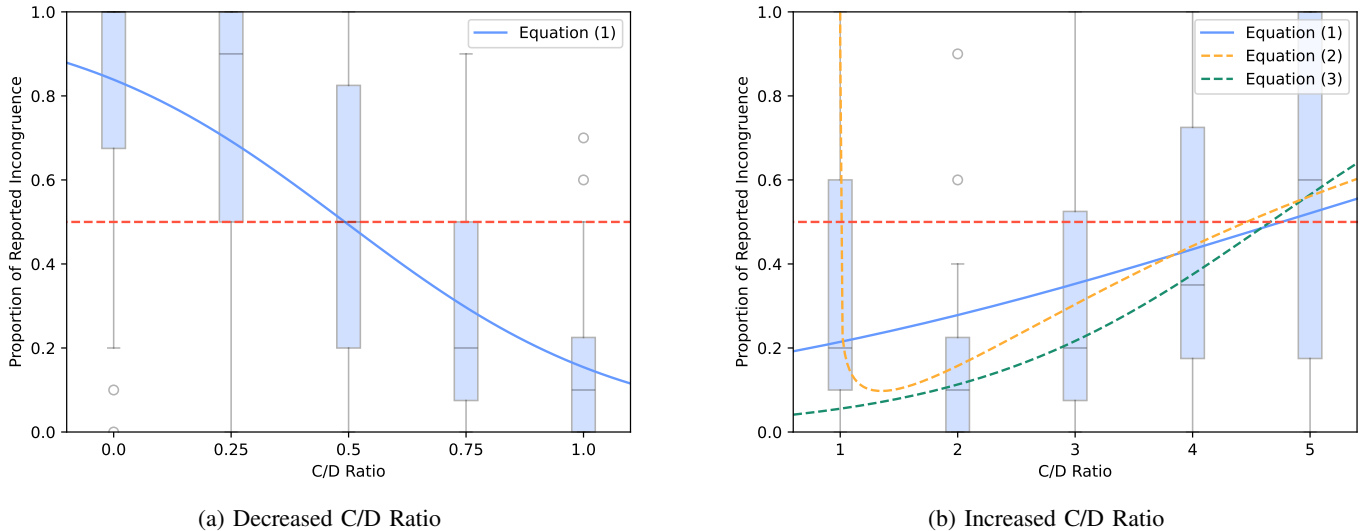


Fig. 2: Proportion of reported incongruence of real and virtual hand movements for (a) decreased and (b) increased C/D RATIO manipulations. The red dotted line describes the detection threshold with a proportion of 0.5. The blue line describes the fitted psychometric function (Equation 1). For increased C/D RATIO, we additionally plot alternative functions for descriptive value as yellow (Equation 2) and green (Equation 3) dotted lines.

are mainly interested in the timeframe of the downward press during which the C/D RATIO manipulations apply increasing offsets, we calculated the average time participants took to press the virtual object until the limit of 30mm was reached, which amounted to ~ 720 ms. Thus, we segmented the data into continuous epochs spanning from 200ms before to 720ms after the start of each press, using the period of -200ms to 0ms as a baseline. We then conducted an independent component analysis (ICA) using the *fastica* algorithm to repair artifacts. Bad epochs were identified by the Autoreject library [52] and fed to the ICA algorithm for a robust fit. Afterward, we ran Autoreject again on the processed data in case of non-stereotypical artifacts and ran a random sample consensus (RANSAC) method of spherical splines [53] to detect and correct possible remaining bad or outlier electrode channels.

IV. RESULTS

In the following, we present the results of our study. We first provide a psychometric analysis of the yes-no paradigm to confirm that our replication aligns with previous findings (subsection IV-A). Next, we report on the EEG preprocessing (III-G) and analysis, which we separated into an analysis of general indicators for subjective incongruence (IV-B), followed by a split analysis based on increased and decreased C/D RATIO, acknowledging these as distinct phenomena (IV-C). We conduct spatio-temporal and frequency analyses for each. Finally, we train Random Forest Classifiers on averaged EEG features to explore their potential for in situ detection of HIs (IV-D).

A. Psychometric Analysis

To validate our study method and allow for comparison to existing psychometric investigations of detection thresholds, we followed the established procedure for analyzing and fitting

psychometric functions for the Method of Constant Stimuli [36, 33, 8, 54, 55]. We calculated the average proportion of reported incongruence for each level of intensity across repetitions and participants. We then fitted psychometric functions to the proportions separately for two blocks of decreased and increased C/D RATIO. We fitted a logistic psychometric function (see [8, 55, 54]) with the following form:

$$f(x) = \frac{1}{1 + e^{ax+b}} \quad \text{for } a, b \in \mathbb{R} \quad (1)$$

Figure 2a and Figure 2b respectively show the fitted psychometric curve for decreased ($a = 3.35, b = -1.65$) and increased ($a = -0.35, b = 1.30$) C/D RATIO as blue lines. We observe a non-monotonous increase in proportion of reported incongruence to increased C/D RATIO analogous to the findings of Weiss et al. [8], where a direct movement mapping (C/D RATIO = 1) is perceived as less congruent than particular amplifications of the movement. Thus, we further fitted the following functions in line with the recommendations of Weiss et al. [8]:

$$w(x) = 1 - a * \left(\frac{k}{\lambda} * \left(\frac{x}{\lambda} \right)^{k-1} * e^{-(x/\lambda)^k} \right) \quad \text{for } a, \lambda, k \in \mathbb{R}^+ \quad (2)$$

$$g(x) = \frac{1}{1 + e^{ax+b}} \quad \text{for } a, b \in \mathbb{R} \text{ and } x > 1. \quad (3)$$

Their resulting curves are displayed in Figure 2b as the yellow (Equation 2, with $\lambda = 4.08, k = 1.08, a = 4.43$) and green (Equation 3, with $a = -0.77, b = 2.84$) dashed lines. The detection threshold (DT) is defined as the stimulus intensity at which participants detect the stimulus 50% of the time. In our experiment, the stimulus corresponds to movement manipulations, and the threshold represents the level of movement amplification that leads to a proportion of reported mismatch of 0.5. Using Equation 1 results in a DT of 0.49 for decreased C/D RATIO and 4.76 for increased C/D RATIO ($DT = 4.46$ for Equation 2, $DT = 4.66$ for Equation 3).

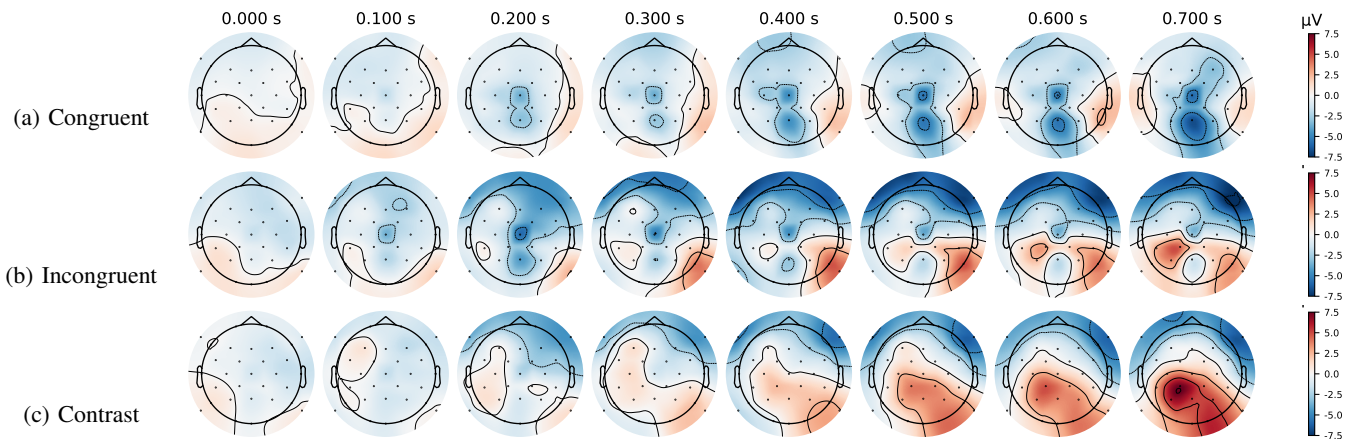


Fig. 3: Power distribution across all 32 channels spanning the duration of the press for subjectively congruent (a) and subjectively incongruent (b) C/D RATIO manipulations, as well as the contrast between them (c).

B. General Correlates to Reported Incongruence

Figure 3 illustrates the power distribution across channels during our investigated timeframes for all subjectively congruent (Figure 3a) and incongruent (Figure 3b) events, as well as the contrast between them (Figure 3c). For detected incongruencies, we observe decreased potentials in the frontal regions compared to subjectively congruent events. Conversely, higher potentials are present in the occipital, parietal, and temporal-parietal regions towards the end of the event.

a) Finding Activity Regions: To narrow down the spatial regions of interest, we first conducted a spatio-temporal analysis of the overall electrical potential distributed over channels and time points, comparing all subjectively congruent and incongruent events. To account for the multiple comparison problems in our high-dimensional data, we conducted a non-parametric cluster-based permutation analysis [56] with F-tests. We set a significance level of $p < .05$. The test revealed a significant difference between the two groups. Figure 4 shows two main clusters, the first being observed in the right frontal and frontal polar electrode locations for most of the event's duration, while the second is surrounding the central-parietal, parietal, and occipital areas closer to the end of the press.

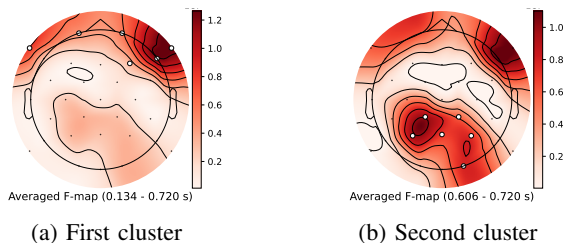


Fig. 4: Primary clusters of differences in activity comparing undetected and detected C/D RATIO manipulations.

b) Frequency Analysis: To further analyze the differences in events, we computed time-frequency representations (TFRs) using complex Morlet wavelets. We focused on the frequency bands delta (0.5 Hz - 4 Hz, in 20 steps), theta (4 Hz - 8 Hz, in 20 steps), alpha (8 Hz - 12 Hz, in 20 steps), and beta

(12 Hz - 30 Hz, in 20 steps). For improved time resolution, the number of cycles was set low at 0.25, 1, 2, and 3 for the delta, theta, alpha, and beta bands, respectively. We applied baseline correction (*ratio*) for each TFR using the -200 ms to 0 ms window. Again, we conducted a non-parametric cluster-based permutation analysis [56] to assess the differences between subjectively congruent and incongruent events within each band and set the significance threshold to $p < .05$. In addition to comparing all identified and unidentified manipulations, we also analyzed each C/D RATIO level separately, contrasting reportedly congruent and incongruent events. This ensures that the observed activity differences reflect neural processes related to manipulation identification rather than visual stimulus changes due to C/D RATIO variations. We conducted a separate analysis of different spatial regions. Our report focuses on the regions identified as having the highest informative value, based on the results of the initial spatio-temporal analysis.

For the electrodes placed over the frontal lobe (F_z , F_3 , F_4 , F_7 , F_8 , F_9 , F_{10}), we found significant differences between subjectively congruent and incongruent events for all investigated frequency bands (delta, theta, alpha, beta). Figure 5a shows the contrast between all subjectively congruent and incongruent events, with significant clusters highlighted. For each band, we can observe a significant cluster towards the end of the press, starting at around 650-700 ms and reaching until the end of the investigated time frame. For the theta, alpha, and beta bands, we additionally observe clusters from \sim 50-250 ms after the start of the press. When analyzing individual C/D RATIO levels, we observed significant differences among frequency bands for C/D RATIO of $0\times$ (in delta and theta at \sim 400 ms), $0.25\times$ (delta, alpha, beta at \sim 400 ms), $1\times$ (delta, theta, alpha at \sim 650 ms), $3\times$ (beta at \sim 650 ms), and $4\times$ (delta, theta, alpha at \sim 100-400 ms and beta at \sim 650 ms).

For the parietal region (P_z , P_3 , P_4 , P_7 , P_8), the test showed a significant difference for all frequency bands. Figure 5b shows the contrast and significant clusters. In the delta and theta bands, we observe a significant cluster centered around \sim 350-450 ms and another significant cluster beyond \sim 650 ms,

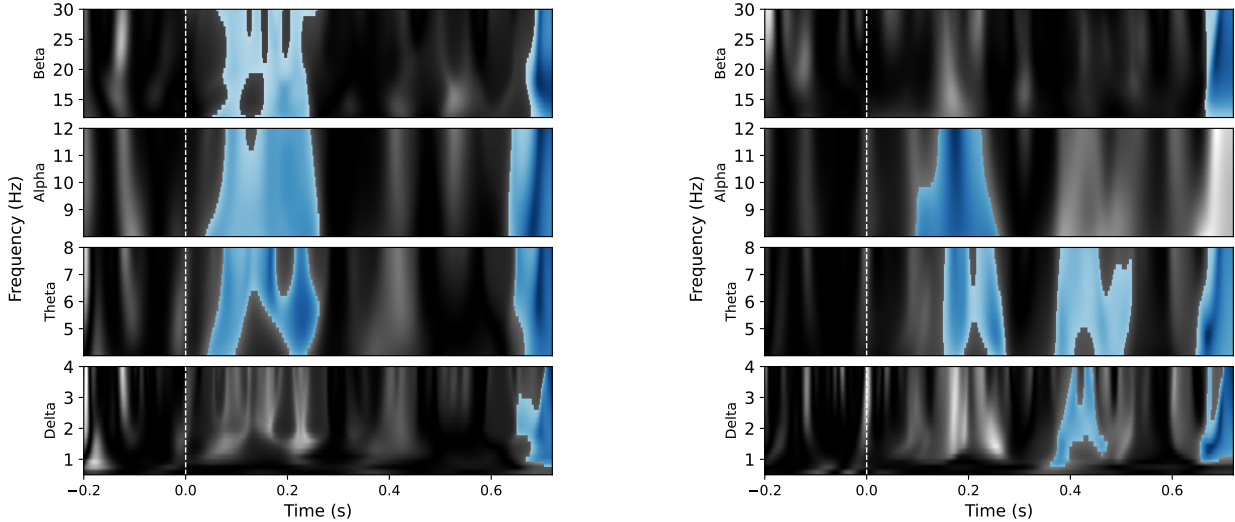
(a) Contrasts in the frontal region ($F_z, F_3, F_4, F_7, F_8, F_9, F_{10}$).(b) Contrasts in the parietal region (P_z, P_3, P_4, P_7, P_8).

Fig. 5: Contrasts between TFRs for all subjectively congruent and incongruent events for electrodes positioned over the frontal region (a) and parietal region (b). The horizontal axis describes time in seconds, with zero being the onset of the press. Lighter areas describe larger contrasts, and significant clusters are highlighted in blue, indicating a significantly stronger negative deflection during reported incongruence.

which is also present in the beta band. Additionally, in the theta band, we observe an earlier cluster between ~ 100 - 150 ms to 300 ms that is correspondingly observed in the alpha band. Separated by levels of C/D RATIO, we found significant differences at $0.25\times$ manipulations (beta at ~ 300 ms) and $3\times$ manipulations (delta at ~ 200 ms, ~ 400 ms and ~ 650 ms, theta at ~ 200 ms, and beta at ~ 200 ms and ~ 600 ms).

Similarly, the test revealed significant differences in all bands over the central-parietal region ($CP1, CP2, CP5, CP6$) between the detected and undetected events. We observe two significant clusters in each band. The first is starting early ~ 50 - 150 ms after stimulus onset and ranging until ~ 200 - 300 ms. The second can be observed towards the end of the press with its onset at ~ 400 ms for the delta and theta bands, ~ 500 ms in the alpha band, and ~ 600 ms in the beta band. These later clusters are all present until the end of the investigated time window. C/D RATIO level-based analysis shows these significant differences to be present for $0.25\times$ (beta at ~ 300 ms), $0.5\times$ (beta at ~ 300 ms), $1\times$ (delta & theta beyond ~ 400 ms, alpha & beta beyond ~ 600 ms), $3\times$ (all bands at ~ 200 ms, delta additionally beyond ~ 600 ms), and $4\times$ amplifications (all bands beyond ~ 600 ms, delta and theta additionally at ~ 100 - 300 ms).

We found further significant differences among all bands for electrodes positioned over the occipital lobe ($Oz, O1, O2$) and frontal-central area ($FC1, FC2, FC5, FC6$). We found a significant difference only in the alpha band for electrodes over the central and temporal ($C3, C4, Cz, T7, T8$) regions and only the delta band for the frontal polar ($Fp1, Fp2$) regions. Individual C/D RATIO-level comparisons similarly exhibit significant contrasts among the occipital (for $0.5\times, 1\times, 2\times, 3\times$, and $4\times$ C/D RATIO), frontal-central (for $1\times, 3\times$, and $4\times$), central and temporal (for $3\times$, and $4\times$), and frontal polar region (for $0\times, 0.25\times$, and $4\times$).

C. Increased & Decreased C/D Ratio

Subsequently, we segmented the data into two blocks: decreased and increased C/D RATIO adjustments. This separation allows us to account for the different phenomena induced by virtually restricting or amplifying hand movements. We present the differences in potentials across channels between reported congruent and incongruent events separately during decreased and increased C/D RATIO adjustments in Figure 6.

Non-parametric cluster-based tests revealed significant differences between events for both the decreased and increased C/D RATIO. Figure 7a and Figure 7b respectively show significantly different clusters in the decreased and increased scenarios. In addition to the significant differences between subjectively congruent and incongruent events for both groups, we can observe a clear separation between the restricted (C/D RATIO < 1) and amplified hand movements (C/D RATIO > 1). The detection of decreased C/D RATIO manipulations resulted in an increased activity largely around the center and right parietal, occipital, and central-parietal regions, as well as the centrally located electrodes above the frontal lobe starting from ~ 380 ms. Increased C/D RATIO manipulations instead exhibited an opposing deflection centered around the right frontal and frontal polar area starting around ~ 120 ms.

a) *Decreased C/D Ratio*: Focusing solely on the events where we decreased C/D RATIO, we again computed TFRs for each frequency band and region using the same decomposition and subsequent cluster-based analysis. The analysis revealed significant differences in the beta bands (12-30 Hz) of the parietal (P_z, P_3, P_4, P_7, P_8), central-parietal ($CP1, CP2, CP5, CP6$), central ($C3, C4, Cz$), and frontal region ($F_z, F_3, F_4, F_7, F_8, F_9, F_{10}$), which we present in Figure 8a. For all of these, we found a significant cluster centered around ~ 300 ms, spanning an area of 50 - 100 ms in width. Further analyses did

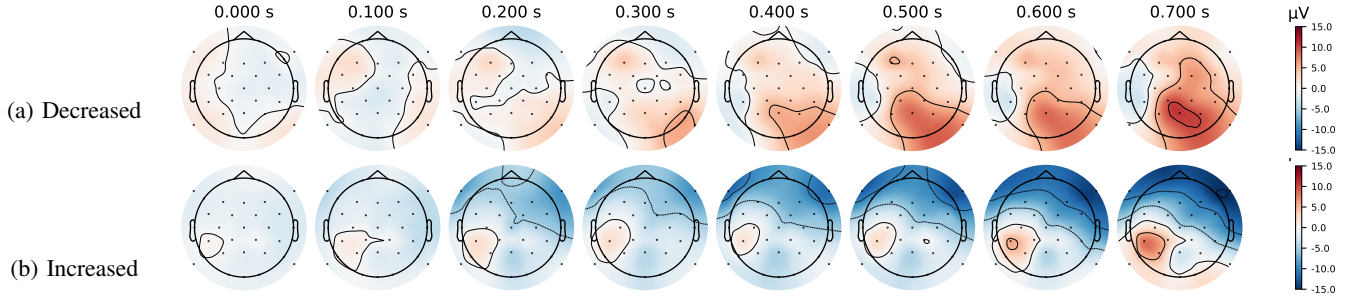


Fig. 6: Activity contrasts between subjectively congruent and incongruent events for decreased (a) and increased (b) C/D RATIO

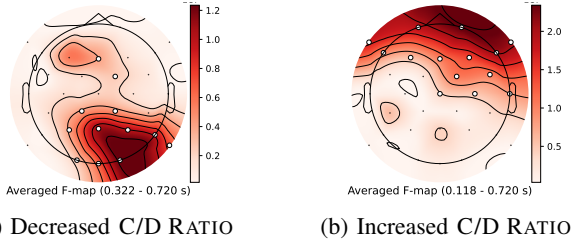


Fig. 7: Main clusters of activity differences between subjectively congruent and incongruent manipulations for decreased (a) and increased (b) C/D RATIO respectively.

not reveal any significant differences in any frequency bands for the occipital (Oz , $O1$, $O2$), frontal-central ($FC1$, $FC2$, $FC5$, $FC6$), or the frontal polar region ($Fp1$, $Fp2$).

b) Increased C/D Ratio: We again computed TFRs for each frequency band and region using the same decomposition and subsequent cluster-based analysis for the events where C/D RATIO was increased.

For the electrodes placed over the frontal lobe (Fz , $F3$, $F4$, $F7$, $F8$, $F9$, $F10$), we found a significant difference between subjectively congruent and incongruent events in all investigated frequency bands (delta, theta, alpha, beta). Contrasts can be observed in Figure 8b. In each band, we observe a significant cluster beginning around 20-100 ms and ending at ~ 300 ms after the start of the press. Additionally, we found another significant cluster in each band emerging around 650-700 ms. For the delta and theta bands, we found an additional cluster spanning from ~ 300 ms to ~ 500 ms.

Similarly, for the electrodes positioned over the frontal-central area ($FC1$, $FC2$, $FC5$, $FC6$), we found significant differences in all bands with large clusters starting right around the start of the press (~ 0 ms). For delta and theta, these clusters span to ~ 500 ms. For alpha and beta, these clusters stop at ~ 300 ms. Additionally, we observe another significant cluster in all bands starting between 600-670 ms.

Additionally, we found significant differences in all bands for the central and temporal ($C3$, $C4$, Cz , $T7$, $T8$), central-parietal ($CP1$, $CP2$, $CP5$, $CP6$), parietal (Pz , $P3$, $P4$, $P7$, $P8$), and occipital (Oz , $O1$, $O2$) regions. For the electrodes located over the frontal polar region ($Fp1$, $Fp2$), we only found a significant difference in alpha and beta with a significant cluster observed from ~ 100 ms to ~ 200 - 250 ms in both bands and an additional cluster in beta starting at ~ 700 ms.

D. Random Forest Classification

The present study primarily aimed to identify EEG correlates of HI detection rather than generating data for machine learning. However, to explore the potential for in situ classification of users' HI detection, we trained Random Forest (RF) classifiers on the collected EEG data. We employed simple averaged EEG features that are independent of precise timing, which, while potentially reducing model performance, provide valuable insights into the potential for adaptive systems where exact event-related measurements are inconsistent.

We first computed the power spectral density (PSD) in each band and electrode using multitaper spectrum estimation [57]. We then calculated the average PSD (in μV) across the entire epoch (0 ms - 720 ms) of each trial. We drop all information regarding C/D RATIO, participant, or repetition to train a binary classifier (subjectively congruent or incongruent) solely on PSD averages. The resulting training matrix contains 3200×160 records. The 3200 rows consist of the 100 trials for each of the 32 participants. Each row consists of 160 columns with the averaged PSD for each of the 32 electrodes for all four bands and a band spanning across all four (*Delta: 0.5-4 Hz, Theta: 4-8 Hz, Alpha: 8-13 Hz, Beta: 13-30 Hz, All: 0.5-30 Hz*). We optimized hyperparameters via grid search and evaluated using 20-fold cross-validation (CV) and 80-20 train-test split. The hyperparameter grid included the number of trees (100-1000), maximum tree depth (5-30), and minimum samples required to split a node (2-16). During cross-validation, the average weighted F1-score was used as the scoring metric to ensure balanced performance across classes. We ran this grid search on the entire dataset as well as splits of only increased or decreased C/D RATIO to account for the detection of these as separate phenomena. Additionally, we trained RF classifiers with these optimized hyperparameters applied to each individual participant separately, as well as with a Leave-One-Participant-Out (LOPO) cross-validation.

We report the performance of the optimal RF models identified through CV, alongside their corresponding weighted F1-scores, in Table I. All models performed significantly better than chance, which corresponds to a weighted F1-score of 0.5. The results indicate that the model trained exclusively on the increased C/D RATIO dataset achieved the highest weighted F1-scores during CV and on the test set, outperforming both the model trained on the decreased C/D RATIO dataset and the model trained on the combined dataset. When trained on in-

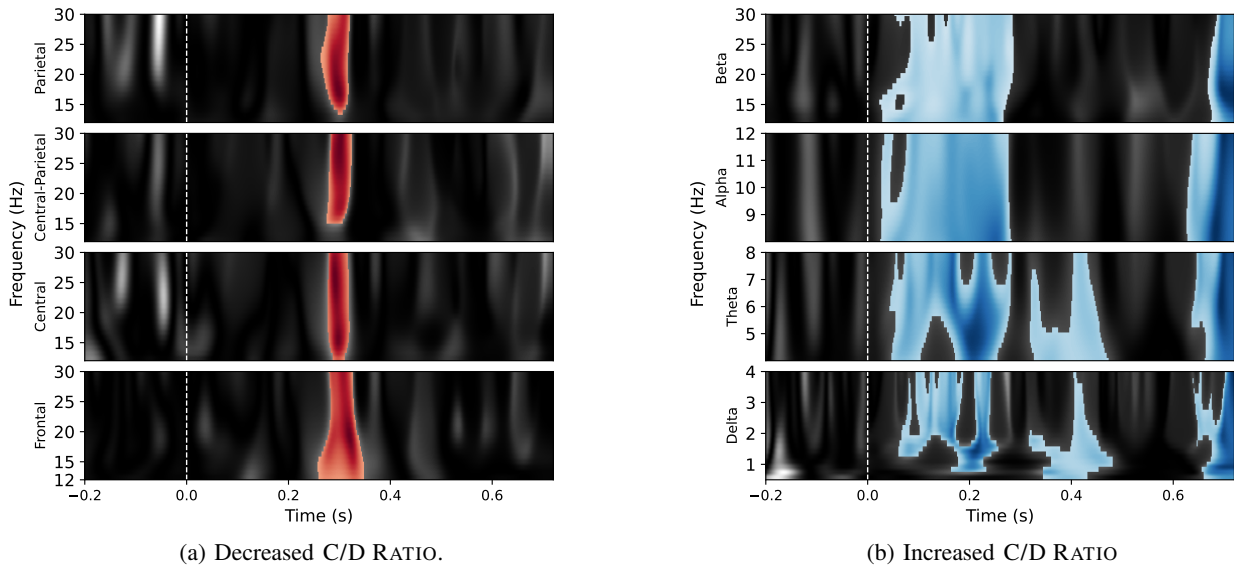


Fig. 8: Contrasts between TFRs for subjectively congruent and incongruent events with decreased C/D RATIO (a) and increased C/D RATIO (b). (a) shows significant differences in the beta band over four different regions. (b) shows significant differences in all bands for the frontal region (Fz , $F3$, $F4$, $F7$, $F8$, $F9$, $F10$). Red and blue, respectively, highlight clusters with significantly stronger positive or negative deflection.

Dataset	Optimal Hyperparameters	20-fold CV F1-W	Test-Set F1-W	Individual Training Mean F1-W (SD)	LOPO Mean F1-W (SD)
Increased	max_depth: 20, min_samples_split: 10, n_estimators: 250	0.68	0.73	0.69 (0.21)	0.54 (0.23)
Decreased	max_depth: 10, min_samples_split: 6, n_estimators: 300	0.66	0.62	0.70 (0.20)	0.47 (0.17)
Combined	max_depth: 25, min_samples_split: 10, n_estimators: 500	0.65	0.63	0.61 (0.17)	0.52 (0.15)

TABLE I: Comparison of Random Forest models based on Weighted F1-scores (F1-W) during 20-fold cross-validation and on the test-set. Additionally, this table presents the mean F1-W (and standard deviation) of training these models on individual participants and using Leave-One-Participant-Out cross-validation.

dividual participants using the same hyperparameters, models trained separately on the increased and decreased C/D RATIO datasets demonstrated better performance compared to the combined dataset, suggesting that separate datasets allow for better participant-specific generalization. In contrast, LOPO cross-validation showed reduced performance across all models. Nonetheless, the model trained on the increased C/D RATIO dataset consistently achieved the highest weighted F1-scores in this evaluation setup.

V. DISCUSSION

Our findings reveal distinct spatiotemporal and time-frequency EEG signatures associated with users' subjective detection of the changes introduced by the HI, and we found that even simple averaged signals can partially separate these patterns. This suggests promising applications for future in situ use. In this section, we discuss the validity of our protocol (subsection V-A) and the insights gained from the combined (V-B) and individually separated phenomena (V-C). We then explore potential origins of the observed signatures and their

implications (V-D, V-E, V-F). Finally, we discuss the feasibility of applying this approach to detect HIs beyond controlled laboratory settings (V-G) and outline future directions to expand its potential and address its limitations (V-H).

A. Psychometrics

We designed our study to follow a standard psychometric approach for finding detection thresholds, ensuring the validity of our measurements. Our analysis showed expected patterns consistent with previous HI research. In line with the findings of Weiss et al. [8], we found reduced movements to be easier to detect than increased ones, with thresholds of 0.49 ($\sim 2\times$ reduction) for decreased and 4.76 for increased ratios. Based on their given approximation function, these thresholds would allow for changes in perceived compliance of -5.5% and +33.8% respectively. We found participants similarly overestimated their hand movements with a C/D RATIO amplification of $2\times$ being judged more frequently to be congruent with actual movements than no manipulation (C/D RATIO = 1). These effects, absent in studies on mid-air hand redirection without

haptic feedback [33], can likely be attributed to the resistance feedback employed [8, 26]. Compared to Weiss et al. [8], our results showed broader boundaries within which the HI remained undetected. This may be partially attributed to the minor differences in study design, such as participants being seated to reduce EEG noise. Previous studies have consistently demonstrated significant individual variations in boundaries for hand redirections [11, 38, 58]. These findings suggest that the observed discrepancies in psychometric results may stem from differences in participant samples, underscoring the importance of addressing these interpersonal deviations.

B. General Indicators of HI Detection

Our findings demonstrate notable activity differences across multiple brain regions and frequency bands associated with the perceived detection of the HI induced incongruence compared to non-detection. In the comparison of all subjectively congruent and incongruent events, regardless of whether the movement was amplified or restricted, significant differences emerged, particularly in the parietal, central-parietal, and occipital regions. Individual comparisons at each C/D RATIO level confirmed that these differences persist across various amplifications, suggesting they result from the discrimination process rather than visual stimulus changes as a confounding factor. When we examined events separately for amplified and restricted movements, distinct patterns appeared for each (see subsection V-C). However, both cases shared similar activity differences in electrodes within the parietal and central-parietal regions, as shown in Figure 6, with notable differences in the beta bands of these areas between events judged to be congruent and incongruent. This consistency in certain brain areas and frequency bands suggests that these regions and bands could serve as reliable indicators for general HI detection, while also highlighting potential areas of interest for distinguishing between the effects of restricted versus amplified hand movements.

C. Signatures of Restricted and Amplified Movement

Previous research [8, 45] has treated restricted and amplified hand movements as distinct phenomena due to differences observed in psychometric outcomes. Our findings provide physiological evidence supporting this distinction, demonstrating that these two phenomena are perceived through separate processes. We identified two distinct EEG signatures in the averaged potentials and time-frequency representations associated with detecting increases or decreases in C/D RATIO. These signatures suggest that separate processes are at play when hand movements are perceived as either restricted or amplified, which can, therefore, be examined independently. In our analysis of subjectively congruent versus subjectively incongruent events across all C/D RATIO conditions, we observed two primary clusters of activity differences (see Figure 4). These clusters are similarly visible when isolating the main activity contrasts for increased (see Figure 7b) and decreased (see Figure 7a) movements.

While general markers of HI detection could support broader applications, addressing these distinct phenomena

separately enhances our ability to fine-tune detection methods, resulting in better adaptability for specific use cases. Amplified movements evoke larger, temporally distributed activity changes, making them detectable with simpler metrics like averaged PSD values (see subsection IV-D). In contrast, restricted movements elicit significant but more transient changes (see Figure 8a), likely requiring advanced methods to account for temporal shifts caused by the continuous HI onset.

D. Visuo-Somatosensory Integration

Our findings revealed increased activity in electrodes positioned over the central to posterior parietal regions, aligning with prior research identifying these areas as critical for multisensory integration. Prior work has repeatedly shown the importance of areas inside the parietal lobe in multisensory integration. For instance, the primary somatosensory cortex (SI) [59, 12] and the posterior parietal cortex (PPC) [12, 60] have consistently been implicated in the integration of visual and somatosensory information. Although our investigation relied on EEG data obtained from surface electrodes, the pronounced activity observed over these regions suggests measurable differences in multisensory integration during reportedly congruent versus incongruent HI manipulations.

The exact mechanisms driving these integration differences remain to be fully understood. The HI introduces multiple factors influencing visuo-somatosensory integration, including tactile and kinesthetic feedback from the haptic device and proprioceptive changes associated with motor tasks. Comparable studies in visuo-tactile stimulation [59, 60], visuo-kinesthetic feedback [12], and visuo-motor tasks [43] have all demonstrated significant activity changes in these regions.

Additionally, our results suggest a slight left-hemisphere dominance in parietal activity, consistent with prior findings that cortices contralateral to the stimulus location exhibit heightened activation during somatosensory stimulation [61]. While the visual stimuli were centrally positioned, the haptic interactions were performed exclusively with the right hand, accounting for this contralateral activation.

E. Error Processing

We observed significant negative potentials in frontal regions during perceived incongruence, particularly under conditions of amplified hand movements. This aligns with prior research identifying the frontal cortex as central to error detection and resolution processes during incongruent cross-modal stimulation [62, 43, 41, 44]. For instance, Savoie et al. [43] reported significant negative deflections during visuo-motor prediction errors in the mid-frontal regions (electrode positioned on Fz , $FC1$, $FC2$) resembling the feedback-related negativity (FRN). FRN is commonly associated with negative feedback stimuli signaling an error or loss, which evokes negative potentials early after stimulus onset originating in the anterior cingulate cortex (ACC) [63]. Further studies have shown that visuo-haptic mismatches [7] and hand redirection [45] evoke similar negative potentials in single electrode (FCz) ERP analyses, suggesting this activity reflects prediction error processing resulting from detected mismatches.

Due to the continuous onset of offset manipulations in our experiment, temporal dynamics of the observed effects are more complex to interpret, as these cannot align neatly with ERPs. We observed significant differences emerging early, rather than solely at the endpoint of the manipulation, which may indicate sensitivity to dynamic movement changes rather than static limb offsets. These early responses indicate a rapid detection of incongruencies in movement dynamics in active (haptic) exploration.

F. Body Ownership

Activity differences in the frontal regions, specifically the premotor cortex, have also been reported in the context of the Rubber Hand Illusion (RHI) [64, 65]. The classical RHI revolves around the integration of an artificial (rubber) limb into one’s own body schema as a result of simultaneous tactile stimulation of a participant’s real hand and visually showing congruent stimulation of the artificial hand [66]. It relies on visuo-tactile integration and resolution of the mismatch of vision and proprioception. This concept forms the basis of virtual hand illusions present in many virtual environments, where hand representations are integrated into the user’s body schema due to congruent prediction and feedback of hand movements, with [67] or without [68] tactile stimulation. Previous research on the RHI [64, 65] has demonstrated increased premotor cortex activity to correlate with the subjective strength of the ownership illusion. Our finding of decreased potential during detected hand movement manipulations may suggest that such manipulations disrupt this integration, leading to reduced activity in these regions compared to undetected manipulations. This aligns with the reported role of perceived visuo-motor congruence in maintaining body ownership in VR [68, 69].

G. EEG-based HI Detection Beyond Controlled Settings

HI’s inherently introduce many confounding factors that induce substantial noise and artifacts into EEG data due to the involvement of multiple simultaneous processes. Our study required, for instance, motor and proprioceptive processing from pressing the virtual object, the sensory processing of haptic resistance through the device, visual processing of the virtual environment, and the multisensory integration of these cues. Together, these confounding factors complicate the physiological measurement of HI effectiveness or detectability. The nonetheless significant differences we found during detection and non-detection highlight the distinct underlying processes that cause large enough effects to be detectable and separable with EEG despite the noise. This ability to separate signals is essential for the potential application of such a system to detect HI’s in real-life contexts, where numerous confounding factors are naturally present.

Our results demonstrate that even relatively simple Random Forest models, trained on a limited dataset due to the exploratory nature of this study, can achieve a degree of separability using basic EEG-derived features, such as average PSD values. This finding highlights the potential for detecting HI’s in situ and establishes a foundation for further research with

more sophisticated models and larger, purpose-built datasets. Additionally, our analysis reveals that separating the increased and decreased C/D RATIO conditions significantly improves model performance compared to treating these phenomena as a combined effect. The superior performance of participant-specific models, combined with the relatively low scores observed in LOPO cross-validation, underscores the importance of personalized calibration. This result suggests that generalized models may be less effective in accommodating individual variability, emphasizing the need for tailored approaches in future EEG-based HI detection systems.

H. Limitations & Future Work

We limited our investigation to spatiotemporal and time-frequency analysis of activity and did not perform an analysis of ERP. This is primarily due to the continuous onset of manipulation of the employed HI, which does not allow for precisely determining when participants detected the HI after pressing. Related research indicates that the resulting signatures likely exhibit irregular patterns compared to typical ERPs [11]. Further, ERPs complicate possible future in situ applications by requiring precise timings of potentials. Nevertheless, previous work has shown ERPs to be a qualified indicator of similar phenomena [7, 38], which could support future approaches to HI detection wherever exact measurements of transient changes are reliable.

Moreover, the variability in HI’s across elicitation methods limits the generalizability of findings from a single experimental setup. As such, our analysis is restricted to correlates within the context of our investigated HI and should serve as a foundation to inform future research in HI detection and evaluation. While our method relies on imperceptible manipulations, many elicitation approaches for HI’s use noticeable stimuli, which may induce response biases in typical subjective measurements. Here, establishing physiological correlates for a wide range of HI’s could help distinguish the objective signatures caused by the original stimulus from those linked to the resulting changes in haptic perception.

Further, due to the large number of comparisons when contrasting events for every individual level of manipulation, our reporting focused largely on contrasts of aggregated events to provide a comprehensive overview. We provide all contrasts in our repository (see section VII).

Lastly, while this study identified strong physiological correlates of the investigated HI, we emphasize that the EEG features presented here are intended to complement, not replace, well-established psychophysical methods — at least until a more robust physiological foundation is established.

VI. CONCLUSION

Our investigation revealed EEG correlates to be a reliable indicator for the detection of HI’s. Through measurements employed during a classical psychophysical study, we found prominent differences in activity during manipulations judged to be congruent compared to incongruent. Particularly, we found major differences in activity and oscillatory signatures above the central and the parietal areas — which comprise

cortices crucial in multisensory integration — and the frontal lobe — which may be indicative of error processing. We trained machine learning models on simple averaged EEG features, which demonstrated the potential for in situ use of EEG-based HI detection. These findings enable the future development of adaptive HI systems that can adjust HI elicitation to fit individual and transient contextual factors, consequently allowing HIs to produce more convincing and robust haptic rendering without compromising users' experiences.

VII. OPEN SCIENCE

We provide our project files, collected datasets, analysis scripts, and analysis results on the Open Science Framework⁷.

REFERENCES

- [1] C. Wee, K. M. Yap, and W. N. Lim, "Haptic Interfaces for Virtual Reality: Challenges and Research Directions," *IEEE Access*, vol. 9, pp. 112 145–112 162, 2021, conference Name: IEEE Access.
- [2] M. O. Ernst and M. S. Banks, "Humans integrate visual and haptic information in a statistically optimal fashion," *Nature*, vol. 415, no. 6870, pp. 429–433, Jan 2002.
- [3] M. O. Ernst and H. H. Bühlhoff, "Merging the senses into a robust percept," *Trends in Cognitive Sciences*, vol. 8, no. 4, pp. 162–169, 2004.
- [4] M. Kurzweg, Y. Weiss, M. O. Ernst, A. Schmidt, and K. Wolf, "Survey on haptic feedback through sensory illusions in interactive systems," *ACM Comput. Surv.*, vol. 56, no. 8, Apr. 2024.
- [5] K. Wolf and T. Bäder, "Illusion of surface changes induced by tactile and visual touch feedback," in *Proceedings of the 33rd Annual ACM Conference Extended Abstracts on Human Factors in Computing Systems*, ser. CHI EA '15. New York, NY, USA: Association for Computing Machinery, 2015, p. 1355–1360.
- [6] E. Bouzbib, C. Pacchierotti, and A. Lécuyer, "When tangibles become deformable: Studying pseudo-stiffness perceptual thresholds in a vr grasping task," *IEEE Transactions on Visualization and Computer Graphics*, vol. 29, no. 5, pp. 2743–2752, 2023.
- [7] L. Gehrke, S. Akman, P. Lopes, A. Chen, A. K. Singh, H.-T. Chen, C.-T. Lin, and K. Gramann, "Detecting visuo-haptic mismatches in virtual reality using the prediction error negativity of event-related brain potentials," in *Proceedings of the 2019 CHI Conference on Human Factors in Computing Systems*, ser. CHI '19. New York, NY, USA: Association for Computing Machinery, 2019, p. 1–11.
- [8] Y. Weiss, S. Villa, A. Schmidt, S. Mayer, and F. Müller, "Using pseudo-stiffness to enrich the haptic experience in virtual reality," in *Proceedings of the 2023 CHI Conference on Human Factors in Computing Systems*, ser. CHI '23. New York, NY, USA: Association for Computing Machinery, 2023.
- [9] M. Samad, E. Gatti, A. Hermes, H. Benko, and C. Parise, "Pseudo-haptic weight: Changing the perceived weight of virtual objects by manipulating control-display ratio," in *Proceedings of the 2019 CHI Conference on Human Factors in Computing Systems*, ser. CHI '19. New York, NY, USA: Association for Computing Machinery, 2019, p. 1–13.
- [10] X. d. Tinguy, C. Pacchierotti, M. Emily, M. Chevalier, A. Guignardat, M. Guillaudeux, C. Six, A. Lécuyer, and M. Marchal, "How different tangible and virtual objects can be while still feeling the same?" in *2019 IEEE World Haptics Conference (WHC)*, 2019, pp. 580–585.
- [11] M. Feick, K. P. Regitz, L. Gehrke, A. Zenner, A. Tang, T. P. Jungbluth, M. Rekrut, and A. Krüger, "Predicting the limits: Tailoring unnoticeable hand redirection offsets in virtual reality to individuals' perceptual boundaries," in *Proceedings of the 37th Annual ACM Symposium on User Interface Software and Technology*, ser. UIST '24. New York, NY, USA: Association for Computing Machinery, 2024.
- [12] H. Alsuradi, W. Park, and M. Eid, "Assessment of eeg-based functional connectivity in response to haptic delay," *Frontiers in Neuroscience*, vol. 16, 2022.
- [13] S. Villa, Y. Weiss, N. Hirsch, and A. Wiethoff, "An examination of ultrasound mid-air haptics for enhanced material and temperature perception in virtual environments," *Proc. ACM Hum.-Comput. Interact.*, vol. 8, no. MHCI, Sep. 2024.
- [14] S. J. Lederman and R. L. Klatzky, "Hand movements: A window into haptic object recognition," *Cognitive Psychology*, vol. 19, no. 3, pp. 342–368, 1987.
- [15] S. Martin and N. Hillier, "Characterisation of the novint falcon haptic device for application as a robot manipulator," in *Australasian Conference on Robotics and Automation (ACRA)*, Citeseer. Sydney, Australia: Australian Robotics and Automation Association, 2009, pp. 291–292.
- [16] V. R. Mercado, M. Marchal, and A. Lecuyer, "'haptics on-demand': A survey on encountered-type haptic displays," *IEEE Transactions on Haptics*, vol. PP, pp. 1–1, 2021.
- [17] S. Villa and S. Mayer, "Cobity: A plug-and-play toolbox to deliver haptics in virtual reality," in *Proceedings of Mensch Und Computer 2022*, ser. MuC '22. New York, NY, USA: Association for Computing Machinery, 2022, p. 78–84.
- [18] I. Choi, E. Ofek, H. Benko, M. Sinclair, and C. Holz, "Claw: A multifunctional handheld haptic controller for grasping, touching, and triggering in virtual reality," in *Proceedings of the 2018 CHI Conference on Human Factors in Computing Systems*, ser. CHI '18. New York, NY, USA: Association for Computing Machinery, 2018, p. 1–13.
- [19] C. Pacchierotti, S. Sinclair, M. Solazzi, A. Frisoli, V. Hayward, and D. Prattichizzo, "Wearable haptic systems for the fingertip and the hand: Taxonomy, review, and perspectives," *IEEE Transactions on Haptics*, vol. 10, no. 4, pp. 580–600, 2017.
- [20] P. Naik, J. Unde, B. Darekar, and S. S. Ohol, "Pneumatic artificial muscle powered exoskeleton," in *Proceedings*

⁷https://osf.io/27bwg/?view_only=3a01dc63444749168fde6a62690b36d3

- of the 2019 4th International Conference on Advances in Robotics, ser. AIR '19. New York, NY, USA: Association for Computing Machinery, 2020.
- [21] R. Hinchet, V. Vechev, H. Shea, O. Hilliges, and E. Zurich, "Dextres: Wearable haptic feedback for grasping in vr via a thin form-factor electrostatic brake," *The 31st Annual ACM Symposium on User Interface Software and Technology*, pp. 901–912, 2018.
- [22] S. V. Salazar, C. Pacchierotti, X. de Tinguy, A. Maciel, and M. Marchal, "Altering the stiffness, friction, and shape perception of tangible objects in virtual reality using wearable haptics," *IEEE Transactions on Haptics*, vol. 13, pp. 167–174, 2020.
- [23] Y. Visell and S. Okamoto, *Vibrotactile Sensation and Softness Perception*. London: Springer London, 2014, pp. 31–47.
- [24] A. Metzger and K. Drewing, "Haptically perceived softness of deformable stimuli can be manipulated by applying external forces during the exploration," *2015 IEEE World Haptics Conference (WHC)*, pp. 75–81, 2015.
- [25] S. J. Lederman and L. A. Jones, "Tactile and haptic illusions," *IEEE Transactions on Haptics*, vol. 4, no. 4, pp. 273–294, 2011.
- [26] A. Lecuyer, S. Coquillart, A. Kheddar, P. Richard, and P. Coiffet, "Pseudo-haptic feedback: can isometric input devices simulate force feedback?" in *Proceedings IEEE Virtual Reality 2000 (Cat. No.00CB37048)*. New York, NY, USA: IEEE, 2000, pp. 83–90.
- [27] M. Azmandian, M. Hancock, H. Benko, E. Ofek, and A. D. Wilson, "Haptic retargeting: Dynamic repurposing of passive haptics for enhanced virtual reality experiences," in *Proceedings of the 2016 CHI Conference on Human Factors in Computing Systems*, ser. CHI '16. New York, NY, USA: Association for Computing Machinery, 2016, p. 1968–1979.
- [28] M. Samad, E. Gatti, A. Hermes, H. Benko, and C. Parise, *Pseudo-Haptic Weight: Changing the Perceived Weight of Virtual Objects By Manipulating Control-Display Ratio*. New York, NY, USA: Association for Computing Machinery, 2019, p. 1–13.
- [29] T. Kawabe and Y. Ujitoko, "Pseudo-haptic heaviness influenced by the range of the c/d ratio and the position of the c/d ratio within a given range," *IEEE Transactions on Haptics*, pp. 1–6, 2023.
- [30] W. Chang, S. Je, M. Pahud, M. Sinclair, and A. Bianchi, "Rendering perceived terrain stiffness in vr via preload variation against body-weight," *IEEE Transactions on Haptics*, pp. 1–6, 2023.
- [31] U. Laessoe, S. Abrahamsen, S. Zepernick, A. Raunsbaek, and C. Stensen, "Motion sickness and cybersickness – sensory mismatch," *Physiology & Behavior*, vol. 258, p. 114015, 2023.
- [32] J. Auda, U. Gruenefeld, and S. Schneegass, "Enabling reusable haptic props for virtual reality by hand displacement," in *Proceedings of Mensch Und Computer 2021*, ser. MuC '21. New York, NY, USA: Association for Computing Machinery, 2021, p. 412–417.
- [33] A. Zenner and A. Krüger, "Estimating detection thresholds for desktop-scale hand redirection in virtual reality," in *2019 IEEE Conference on Virtual Reality and 3D User Interfaces (VR)*. New York, NY, USA: IEEE, 2019.
- [34] B. Geslain, S. Besga, F. Lebrun, and G. Bailly, "Generalizing the hand redirection function in virtual reality," in *Proceedings of the 2022 International Conference on Advanced Visual Interfaces*, ser. AVI 2022. New York, NY, USA: Association for Computing Machinery, 2022.
- [35] M. Feick, A. Zenner, O. Ariza, A. Tang, C. Biyikli, and A. Krüger, "Turn-it-up: Rendering resistance for knobs in virtual reality through undetectable pseudo-haptics," in *Proceedings of the 36th Annual ACM Symposium on User Interface Software and Technology*, ser. UIST '23. New York, NY, USA: Association for Computing Machinery, 2023.
- [36] L. A. Jones and H. Z. Tan, "Application of psychophysical techniques to haptic research," *IEEE Transactions on Haptics*, vol. 6, no. 3, pp. 268–284, 2013.
- [37] A. Lecuyer, J.-M. Burkhardt, S. Coquillart, and P. Coiffet, "'boundary of illusion': an experiment of sensory integration with a pseudo-haptic system," in *Proceedings IEEE Virtual Reality 2001*, 2001, pp. 115–122.
- [38] M. Feick, K. P. Regitz, A. Tang, and A. Krüger, "Designing visuo-haptic illusions with proxies in virtual reality: Exploration of grasp, movement trajectory and object mass," in *Proceedings of the 2022 CHI Conference on Human Factors in Computing Systems*, ser. CHI '22. New York, NY, USA: Association for Computing Machinery, 2022.
- [39] A. Halbig and M. E. Latoschik, "A systematic review of physiological measurements, factors, methods, and applications in virtual reality," *Frontiers in Virtual Reality*, vol. 2, 2021.
- [40] F. Chiossi, Y. Weiss, T. Steinbrecher, C. Mai, and T. Kosch, "Mind the visual discomfort: Assessing event-related potentials as indicators for visual strain in head-mounted displays," in *2024 IEEE International Symposium on Mixed and Augmented Reality (ISMAR)*, 2024, pp. 150–159.
- [41] F. Göschl, U. Friese, J. Daume, P. König, and A. K. Engel, "Oscillatory signatures of crossmodal congruence effects: An EEG investigation employing a visuotactile pattern matching paradigm," *Neuroimage*, vol. 116, pp. 177–186, Aug. 2015.
- [42] H. Alsuradi, W. Park, and M. Eid, "Midfrontal theta oscillation encodes haptic delay," *Scientific Reports*, vol. 11, no. 1, p. 17074, Aug 2021.
- [43] F.-A. Savoie, F. Thénault, K. Whittingstall, and P.-M. Bernier, "Visuomotor prediction errors modulate eeg activity over parietal cortex," *Scientific Reports*, vol. 8, no. 1, p. 12513, Aug 2018.
- [44] P. Arrighi, L. Bonfiglio, F. Minichilli, N. Cantore, M. C. Carboncini, E. Piccotti, B. Rossi, and P. Andre, "EEG theta dynamics within frontal and parietal cortices for error processing during reaching movements in a prism adaptation study altering visuo-motor predictive planning," *PLoS One*, vol. 11, no. 3, p. e0150265, Mar. 2016.
- [45] M. Feick, K. P. Regitz, A. Tang, T. Jungbluth, M. Rekrut,

- and A. Krüger, “Investigating noticeable hand redirection in virtual reality using physiological and interaction data,” in *2023 IEEE Conference Virtual Reality and 3D User Interfaces (VR)*. New York, NY, USA: IEEE, 2023, pp. 194–204.
- [46] X. de Tinguy, C. Pacchierotti, M. Marchal, and A. Lécuyer, “Enhancing the stiffness perception of tangible objects in mixed reality using wearable haptics,” *2018 IEEE Conference on Virtual Reality and 3D User Interfaces (VR)*, pp. 81–90, 2018.
- [47] A. Lécuyer, J.-M. Burkhardt, and L. Etienne, “Feeling bumps and holes without a haptic interface: The perception of pseudo-haptic textures,” in *Proceedings of the SIGCHI Conference on Human Factors in Computing Systems*, ser. CHI ’04. New York, NY, USA: Association for Computing Machinery, 2004, p. 239–246.
- [48] M. Rietzler, G. Haas, T. Dreja, F. Geiselhart, and E. Rukzio, “Virtual muscle force: Communicating kinesthetic forces through pseudo-haptic feedback and muscle input,” in *Proceedings of the 32nd Annual ACM Symposium on User Interface Software and Technology*, ser. UIST ’19. New York, NY, USA: Association for Computing Machinery, 2019, p. 913–922.
- [49] A. Gramfort, M. Luessi, E. Larson, D. A. Engemann, D. Strohmeier, C. Brodbeck, R. Goj, M. Jas, T. Brooks, L. Parkkonen, and M. S. Hämäläinen, “MEG and EEG data analysis with MNE-Python,” *Frontiers in Neuroscience*, vol. 7, no. 267, pp. 1–13, 2013.
- [50] A. de Cheveigné and I. Nelken, “Filters: When, why, and how (not) to use them,” *Neuron*, vol. 102, no. 2, pp. 280–293, 2019.
- [51] D. J. Acunzo, G. MacKenzie, and M. C. van Rossum, “Systematic biases in early erp and erf components as a result of high-pass filtering,” *Journal of Neuroscience Methods*, vol. 209, no. 1, pp. 212–218, 2012.
- [52] M. Jas, D. A. Engemann, Y. Bekhti, F. Raimondo, and A. Gramfort, “Autoreject: Automated artifact rejection for meg and eeg data,” *NeuroImage*, vol. 159, pp. 417–429, 2017.
- [53] N. Bigdely-Shamlo, T. Mullen, C. Kothe, K.-M. Su, and K. A. Robbins, “The prep pipeline: standardized preprocessing for large-scale eeg analysis,” *Frontiers in Neuroinformatics*, vol. 9, 2015.
- [54] F. Steinicke, G. Bruder, J. Jerald, H. Frenz, and M. Lappe, “Estimation of detection thresholds for redirected walking techniques,” *IEEE transactions on visualization and computer graphics*, vol. 16, no. 1, pp. 17–27, 2010.
- [55] P. Abtahi and S. Follmer, “Visuo-haptic illusions for improving the perceived performance of shape displays,” in *Proceedings of the 2018 CHI Conference on Human Factors in Computing Systems*, ser. CHI ’18. New York, NY, USA: Association for Computing Machinery, 2018, p. 1–13.
- [56] E. Maris and R. Oostenveld, “Nonparametric statistical testing of eeg- and meg-data,” *Journal of Neuroscience Methods*, vol. 164, no. 1, pp. 177–190, 2007.
- [57] D. Slepian, “Prolate spheroidal wave functions, fourier analysis, and uncertainty — v: the discrete case,” *The Bell System Technical Journal*, vol. 57, no. 5, pp. 1371–1430, 1978.
- [58] J. Hartfill, J. Gabel, L. Kruse, S. Schmidt, K. Riebandt, S. Kühn, and F. Steinicke, “Analysis of detection thresholds for hand redirection during mid-air interactions in virtual reality,” in *Proceedings of the 27th ACM Symposium on Virtual Reality Software and Technology*, ser. VRST ’21. New York, NY, USA: Association for Computing Machinery, 2021.
- [59] N. Kanayama, K. Kimura, and K. Hiraki, “Cortical EEG components that reflect inverse effectiveness during visuotactile integration processing,” *Brain Res*, vol. 1598, pp. 18–30, Dec. 2014.
- [60] G. Gentile, V. I. Petkova, and H. H. Ehrsson, “Integration of visual and tactile signals from the hand in the human brain: An fmri study,” *Journal of Neurophysiology*, vol. 105, no. 2, pp. 910–922, 2011, PMID: 21148091.
- [61] A. Korvenoja, J. Huttunen, E. Salli, H. Pohjonen, S. Martinkauppi, J. M. Palva, L. Lauronen, J. Virtanen, R. J. Ilmoniemi, and H. J. Aronen, “Activation of multiple cortical areas in response to somatosensory stimulation: Combined magnetoencephalographic and functional magnetic resonance imaging,” *Human Brain Mapping*, vol. 8, no. 1, pp. 13–27, 1999.
- [62] M. X. Cohen and T. H. Donner, “Midfrontal conflict-related theta-band power reflects neural oscillations that predict behavior,” *J. Neurophysiol.*, vol. 110, no. 12, pp. 2752–2763, Dec. 2013.
- [63] T. U. Hauser, R. Iannaccone, P. Stämpfli, R. Drechsler, D. Brandeis, S. Walitza, and S. Brem, “The feedback-related negativity (frn) revisited: New insights into the localization, meaning and network organization,” *NeuroImage*, vol. 84, pp. 159–168, 2014.
- [64] H. H. Ehrsson, C. Spence, and R. E. Passingham, “That’s my hand! activity in premotor cortex reflects feeling of ownership of a limb,” *Science*, vol. 305, no. 5685, pp. 875–877, Aug. 2004.
- [65] H. H. Ehrsson, N. P. Holmes, and R. E. Passingham, “Touching a rubber hand: Feeling of body ownership is associated with activity in multisensory brain areas,” *J. Neurosci.*, vol. 25, no. 45, pp. 10564–10573, Nov. 2005.
- [66] M. Botvinick and J. Cohen, “Rubber hands ‘feel’ touch that eyes see,” *Nature*, vol. 391, no. 6669, pp. 756–756, Feb 1998.
- [67] D. Pittera, E. Gatti, and M. Obrist, *I’m Sensing in the Rain: Spatial Incongruity in Visual-Tactile Mid-Air Stimulation Can Elicit Ownership in VR Users*. New York, NY, USA: Association for Computing Machinery, 2019, p. 1–15.
- [68] M. V. Sanchez-Vives, B. Spanlang, A. Frisoli, M. Bergamasco, and M. Slater, “Virtual hand illusion induced by visuomotor correlations,” *PLOS ONE*, vol. 5, no. 4, pp. 1–6, 04 2010.
- [69] K. Kilteni, J.-M. Normand, M. V. Sanchez-Vives, and M. Slater, “Extending body space in immersive virtual reality: A very long arm illusion,” *PLOS ONE*, vol. 7, no. 7, pp. 1–15, 07 2012.



Yannick Weiss received the M.Sc. degree in Human-Computer Interaction in 2021 from LMU Munich in Germany, where he is currently pursuing the Ph.D. degree at the chair of Human-Centered Ubiquitous Media. His research focuses on haptic perception in extended reality scenarios, from uncovering the underlying processes of multisensory perception to creating and adapting haptic experiences for virtual and augmented environments.



Albrecht Schmidt is a professor of computer science at Ludwig-Maximilians-Universität (LMU) in Munich, where he holds a chair for Human-Centered Ubiquitous Media. His research interests are in human-computer interaction, human-centered artificial intelligence, intelligent interactive systems, ubiquitous computing, digital media technologies, and media informatics. He studied computer science in Ulm and Manchester and in 2003 he completed his PhD at Lancaster University. Albrecht chaired the technical program of ACM SIGCHI 2014, he is

on the editorial board of the ACM TOCHI journal, and he is the co-founder of the ACM conference TEI and Automotive User interfaces. In 2018 he was inducted into the ACM SIGCHI Academy, in 2020 he was elected into Leopoldina, the Germany academy of science, and he was named ACM Fellow in 2023.



Steeven Villa is a Computer Scientist and Mechatronic Engineer currently completing his Ph.D. in the Human-Centered Ubiquitous Media group at LMU Munich. His research focuses on human-computer interaction and human augmentation, with particular interest in haptic perception in virtual reality and embodied systems. He investigates how technologies such as electrical muscle stimulation and other haptic modalities can support or extend human sensory, cognitive, and motor functions. His work combines user-centered design, experimental

studies, and system prototyping to explore the effects of interactive technologies on human capabilities. Drawing from computer science, cognitive science, and engineering, his research contributes to the development of systems for VR, robotics, and human augmentation. He holds a B.Sc. from ITM Medellín and an M.Sc. from UFRGS Brazil.